Heteroatom Chemistry
Volume 6, Number 4, 1995

Crystal and Molecular Structures of Diastereomeric 2-Phosphoryl-, 2-Thiophosphoryl-, and 2-Selenophosphoryl-Substituted 1,3-Dithianes

Michał W. Wieczorek, Grzegorz D. Bujacz, and Wiesław R. Majzner

Technical University, Institute of Technical Biochemistry, Stefanowskiego 4/10, 90-924 Łódź, Poland

Piotr P. Graczyk and Marian Mikołajczyk*

Centre of Molecular and Macromolecular Studies, Polish Academy of Sciences, Department of Organic Sulfur Compounds, Sienkiewicza 112, 90-362 Łódź, Poland

Received 11 October 1994; revised 17 January 1995

ABSTRACT

The crystal and molecular structures of five pairs of diastereomeric cis- and trans-2-phosphoryl-, 2-thiophosphoryl-, and 2-selenophosphoryl-5-t-butyl-1,3-dithianes have been determined.

For all the examined compounds, all of the basic geometrical parameters, such as bond lengths, bond and torsion angles, and the deformation of a chair conformation of the six-membered heterocyclic rings, have been established. The differences in corresponding bond lengths and valence angles in diastereomeric cis- and trans-2-P-substituted 1,3-dithianes are discussed.

INTRODUCTION

Considerable efforts have been devoted toward the understanding of the stereoelectronic effects involving second- [1] and third-row [2] atoms. Among them, the S–C–P anomeric interactions recently attracted considerable attention [3,4], and their nature is still a matter of debate.

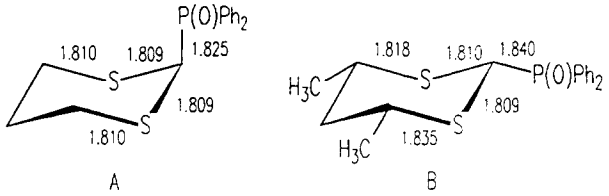

FIGURE 1 Bond lengths in (A) axial and (B) equatorial 2-diphenylphosphinoyl-1,3-dithianes [8].

In general, the changes in bond lengths and angles are thought to be connected with stereoelectronic factors responsible for the observed anomeric effect [5]. This point of view seems to be supported for first-row atoms both by calculations [6] and experiments [7]. However, when second-row atoms are involved in the anomeric interaction, the situation is not so clear. In particular, the initial studies by Juaristi *et al.* on the crystal structure of each of the 2-diphenylphosphinoyl-1,3-dithianes A [8a] and B [8b] (see Figure 1) showed no expected difference between the axial and equatorial C(2)–P bond lengths. Even more, the equa-

Dedicated to Prof. Shigeru Oae on the occasion of his seventy-fifth birthday.

*To whom correspondence should be addressed.

1042-7163/95/$5.00 + .25

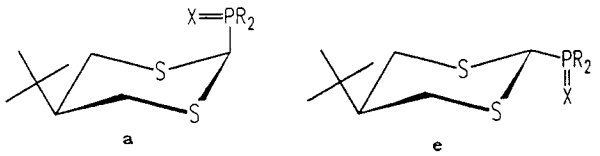

$R_2P{=}X$	$Ph_2P{=}O$	$Ph_2P{=}S$	$Ph_2P{=}Se$	$(OMe)_2P{=}O$	$(CF_3CH_2O)_2P{=}O$
Compound	1a, e	2a, e	3a, e	4a, e	5a, e

FIGURE 2 Structures of 1,3-dithianes determined by X-ray crystallography.

torial C(2)–P bond in B was longer than the axial one, in disagreement with the expectations based on the $n_S - \sigma^*_{C-P}$ negative hyperconjugation.

In the course of our studies [9] on dithioacetals of formylphosphonates, we found the operation of the anomeric effect for the dimethoxyphosphoryl group [$-P(O)(OMe)_2$] connected with the anomeric carbon atom of the 1,3-dithiane [10] and 1,3,5-trithiane [11] rings. Soon afterword, this effect was also shown for the diphenylthiophosphinoyl and diphenylselenophosphinoyl groups at the C(2) atom of the 1,3,5-trithiane [4c,12] and 1,3-dithiane [4a,c] rings.

In order to reveal the characteristic features, which could be attributed to the observed S–C–P anomeric interactions, we decided to study diastereoisomeric 5-*t*-butyl-1,3-dithiane derivatives **1a, e–5a, e** (Figure 2) by means of X-ray crystallography.

Thus, we expected that the comparison of **4a, e** and **5a, e** would reveal the structural changes arising from a more electron-withdrawing character of the P-containing group. On the other hand, the studies on **1a, e–3a, e** were necessary, as far as the importance of destabilizing interactions [4b] (*overlap repulsion*) is concerned.

In this paper, we would like to present full results of our X-ray studies on these compounds and discuss some of the observed structural parameters. As the nature of the anomeric effect operating in 2-P-substituted 1,3-dithianes [1–5] and its effect on the endocyclic S–C and exocyclic C–P bond lengths have been described in detail in our previous paper [13], the present discussion is focused on comparison of the geometry and conformation of the compounds investigated.

RESULTS AND DISCUSSION

The dithianes **1–5** can be compared in a twofold way:

(a) as a series of the compounds with different substituents P = X, X = O, S, Se; and

(b) as pairs of diastereomers with the axial and equatorial position, respectively, of the P = X group.

The 1,3-dithiane rings in all 10 compounds **1a, e–5a, e** adopt a chair conformation each with a different degree of deformation. The corresponding torsion angles and asymmetry parameters as well as the established conformations of the six-membered heterocyclic rings are depicted in Table 1.

A comparison of the values of the torsion angles given in Table 1, for axial and equatorial diastereomers, reveals that the average absolute values of the torsion angles S–C2–S–C are greater in equatorial diastereomers **1–5**. The smallest difference is observed for **4** (4.9°), and it increases on going from **1** to **3**, being the biggest in the latter case (16.9°). In thiophosphoryl and selenophosphoryl compounds (**2** and **3**), this value is greater than in phosphoryl ones (**1**, **4** and **5**).

As a consequence of significantly smaller absolute values of the torsion angles S3–C2–S1–C1 and S1–C2–S3–C4 in axial diastereomers, one observes a distinct deformation of their dithiane rings. In all 10 compounds investigated, the only one of six asymmetry parameters is of a very low value, which indicates the existence of an almost ideal plane of symmetry passing through the C2 and C5 atoms; the other five asymmetry parameters have considerably higher values.

The equatorial arrangement of the P7–C2 bond does not have significant influence on the deformation of a chair conformation. Therefore, the dihedral angles α and β given in Figure 3 have similar values, and the values of asymmetry parameters of the dithiane rings are generally smaller.

The dihedral angles α and β of heterocyclic six-membered rings (Figure 3) and the calculated distances of some atoms from least-squares planes of interest demonstrate further the relationship between the ring conformation and the axial or equatorial position of the $R_2P = X$ group.

In the case of axial diastereomers **1a–5a**, the greatest distance of phosphorus from the basic plane of the ring (least-squares plane through S1, S3, C4, C6 atoms) is observed for **1a** and **4a**. These distances are equal to 2.579(1) Å and 2.577(1) Å), respectively. On the other hand, the smallest distance of 2.491(1) Å is observed for **5a** with the trifluoroethoxy groups bonded to phosphorus. A similar dependence is observed for the dihedral angle α (see Figure 3), which is greatest in **4a** and smallest in **5a**.

An inspection of the corresponding calculated parameters for equatorial diastereomers **1e–5e** reveals that the most distant phosphorus atoms from the ring basic plane is in **1e** (1.381(1) Å), and the smallest distance is observed for **5e** (0.974(1) Å).

The arrangement of the *tert*-butyl group with respect to the least-squares plane passing through the four central atoms (S1, S3, C4, C6) of the heterocyclic ring is defined by the dihedral angle β

TABLE 1 Torsional Angles and Asymmetry Parameters for *cis* and *trans* Dithianes **1–5**

Compound	Torsion angles	Asymmetry parameters	Conformation
1a. $C_{20}H_{25}OPS_2$ O═PPh$_2$ 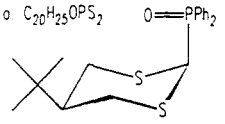	-59.2(2) C_6—S_1 52.0(1); 69.2(2) C_5; C_2; -69.0(2) C_4—S_3 -51.8(1); 58.8(2)	ΔC_s^{S1}=12.4(3) ΔC_2^{S1-C2}= 9.1(3) ΔC_s^{C2}= 0.3(3) ΔC_2^{C2-S3}= 8.4(3) ΔC_s^{S3}=12.1(3) ΔC_2^{S3-C4}=17.2(3) $\lvert\omega\rvert_{av}$=60.0(2)	deformed chair
1e. $C_{20}H_{25}OPS_2$ 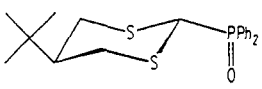	-62.9(2) C_6—S_1 64.8(1); 65.6(2) C_5; C_2; -64.8(2) C_4—S_3 -64.2(1); 61.4(2)	ΔC_s^{S1}= 2.4(4) ΔC_2^{S1-C2}= 3.1(4) ΔC_s^{C2}= 1.0(4) ΔC_2^{C2-S3}= 2.7(4) ΔC_s^{S3}= 2.2(3) ΔC_2^{S3-C4}= 0.7(4) $\lvert\omega\rvert_{av}$=64.0(2)	almost ideal chair
2a. $C_{20}H_{25}PS_3$ S═PPh$_2$ 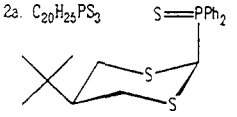	-57.1(3) C_6—S_1 47.2(2); 70.2(3) C_5; C_2; -69.9(3) C_4—S_3 -47.0(2); 56.6(3)	ΔC_s^{S1}=16.5(5) ΔC_2^{S1-C2}=12.0(5) ΔC_s^{C2}= 0.4(5) ΔC_2^{C2-S3}=11.2(5) ΔC_s^{S3}=16.1(5) ΔC_2^{S3-C4}=22.9(5) $\lvert\omega\rvert_{av}$=58.0(3)	deformed chair
2e. $C_{20}H_{25}PS_3$ 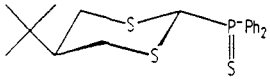	-61.4(2) C_6—S_1 63.2(2); 64.0(3) C_5; C_2; -63.6(3) C_4—S_3 -63.8(2); 61.7(2)	ΔC_s^{S1}= 1.5(4) ΔC_2^{S1-C2}= 2.4(4) ΔC_s^{C2}= 0.4(4) ΔC_2^{C2-S3}= 1.9(4) ΔC_s^{S3}= 1.9(4) ΔC_2^{S3-C4}= 0.6(4) $\lvert\omega\rvert_{av}$=63.0(2)	almost ideal chair
3a. $C_{20}H_{25}PS_2Se$ Se═PPh$_2$ 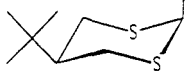	-57.8(3) C_6—S_1 46.6(3); 70.1(4) C_5; C_2; -67.9(4) C_4—S_3 -45.8(3); 54.9(3)	ΔC_s^{S1}=17.2(6) ΔC_2^{S1-C2}=13.7(6) ΔC_s^{C2}= 2.1(6) ΔC_2^{C2-S3}= 9.3(6) ΔC_s^{S3}=15.2(6) ΔC_2^{S3-C4}=22.8(6) $\lvert\omega\rvert_{av}$=57.2(3)	deformed chair
3e. $C_{20}H_{25}PS_2Se$ 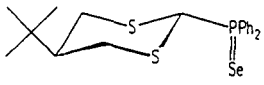	-61.7(2) C_6—S_1 62.5(1); 64.6(3) C_5; C_2; -64.5(3) C_4—S_3 -63.6(2); 62.4(2)	ΔC_s^{S1}= 1.4(4) ΔC_2^{S1-C2}= 2.1(4) ΔC_s^{C2}= 0.8(3) ΔC_2^{C2-S3}= 2.0(3) ΔC_s^{S3}= 2.2(4) ΔC_2^{S3-C4}= 1.7(4) $\lvert\omega\rvert_{av}$=63.2(2)	almost ideal chair
4a. $C_{10}H_{21}O_3PS_2$ O═P(OMe)$_2$ 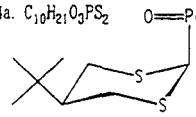	-58.2(3) C_6—S_1 55.6(3); 64.6(4) C_5; C_2; -65.3(4) C_4—S_3 -56.0(2); 59.2(3)	ΔC_s^{S1}= 6.3(6) ΔC_2^{S1-C2}= 4.1(6) ΔC_s^{C2}= 0.8(6) ΔC_2^{C2-S3}= 5.7(6) ΔC_s^{S3}= 7.0(6) ΔC_2^{S3-C4}= 9.2(6) $\lvert\omega\rvert_{av}$=59.8(3)	deformed chair
4e. $C_{10}H_{21}O_3PS_2$ 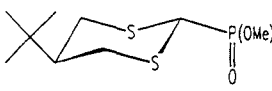	-62.4(3) C_6—S_1 61.0(2); 68.2(4) C_5; C_2; -68.5(4) C_4—S_3 -60.4(3); 62.0(3)	ΔC_s^{S1}= 5.9(6) ΔC_2^{S1-C2}= 4.6(6) ΔC_s^{C2}= 0.5(6) ΔC_2^{C2-S3}= 4.4(6) ΔC_s^{S3}= 5.6(6) ΔC_2^{S3-C4}= 7.7(7) $\lvert\omega\rvert_{av}$=63.8(3)	deformed chair
5a. $C_{12}H_{19}O_3PS_2F_6$ O═P(CH$_2$CF$_3$)$_2$ 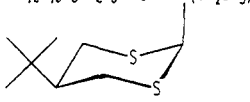	-58.0(2) C_6—S_1 47.4(2); 73.8(2) C_5; C_2; -73.9(2) C_4—S_3 -47.6(2); 58.3(2)	ΔC_s^{S1}=18.7(4) ΔC_2^{S1-C2}=13.2(4) ΔC_s^{C2}= 0.2(4) ΔC_2^{C2-S3}=13.6(4) ΔC_s^{S3}=18.9(4) ΔC_2^{S3-C4}=26.4(4) $\lvert\omega\rvert_{av}$=59.8(2)	deformed chair
5e. $C_{12}H_{19}O_3PS_2F_6$ 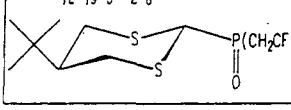	-61.8(2) C_6—S_1 58.0(2); 70.9(2) C_5; C_2; -70.2(2) C_4—S_3 -58.0(2); 61.1(2)	ΔC_s^{S1}= 9.4(4) ΔC_2^{S1-C2}= 7.4(4) ΔC_s^{C2}= 0.6(4) ΔC_2^{C2-S3}= 6.3(4) ΔC_s^{S3}= 9.0(4) ΔC_2^{S3-C4}=12.6(4) $\lvert\omega\rvert_{av}$=63.3(2)	deformed chair

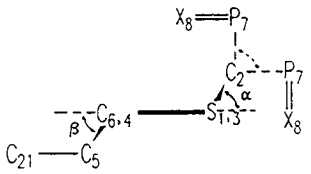

	α(°)	β(°)
1a	51.1(1)	59.2(2)
2a	46.1(2)	60.1(2)
3a	45.3(2)	58.8(2)
4a	55.0(2)	55.7(3)
5a	46.9(2)	63.8(2)
1e	64.6(1)	55.9(2)
2e	63.3(1)	54.5(2)
3e	62.9(1)	55.1(1)
4e	60.6(2)	58.8(2)
5e	58.0(2)	60.6(2)

FIGURE 3 Characteristic dihedral angles of 1,3-dithiane rings in **1–5**.

(Figure 3). It can be seen that the values of β are, in general, greater for axial diastereomers.

The next interesting difference between axial and equatorial diastereomers is the value of (β-α), which describes a flattening of a chair conformation of the six-membered ring. This value varies from 8.1° to 16.9° in the axial compounds (**1a–5a**). In the case of the equatorial compounds (**1e–5e**), this flattening is generally much smaller and ranges from 2.6° to 8.8° (see Figure 3). The exception is the compound **4**, for which both axial and equatorial diastereomers are characterized by very small (β-α) values: 0.7 and 1.8°, respectively.

The interatomic distance S1–S3, which describes the "gaping" of the ring, is almost constant for the equatorial compounds **1e–4e** and equals 2.990–2.998 Å. In compound **5e**, this value is slightly greater and is equal to 3.042 Å. In the axial compounds (**1a–5a**), the S1–S3 distance is generally much greater and ranges from 3.030 Å to 3.065 Å, with the exception of **4a**, where it is 3.003 Å.

The differences between geometrical parameters in axial and equatorial diastereomers discussed above are mainly due to steric (increase of the size of the R_2P=X group on going from X = O to S and to Se) and stereoelectronic effects. The latter have been discussed in a previous paper [13].

The Newman projections around the C2–P7 bond (Figure 4) show the arrangement of the S1, S3, and H21 atoms with respect to oxygen, sulfur, and selenium atoms of the P=X group. In the axial compounds, the H21 atom is always antiperiplanar to these P=X heteroatoms. The respective torsion angles are equal to 169(2), 173(2), 174(2), 179(4), and 178(3)°, respectively, for **1a** to **5a**. Interestingly, this torsion angle (H21–C2–P7–X8, X = O, S, Se) increases in the order **1a**→**2a**→**3a**, thus indicating its dependence on the size of the P = X substituent.

The equatorial position of the phosphoryl group P7=O8 and, additionally, the small size of the phosphoryl oxygen in **1e** are the reasons for the antiperiplanar position of the H21 atom with respect to oxygen, with a torsion angle of 170.2(1)°. In the case of the bigger thio- and selenophosphoryl groups (S in **2e** and Se in **3e**), one observes twisting of the

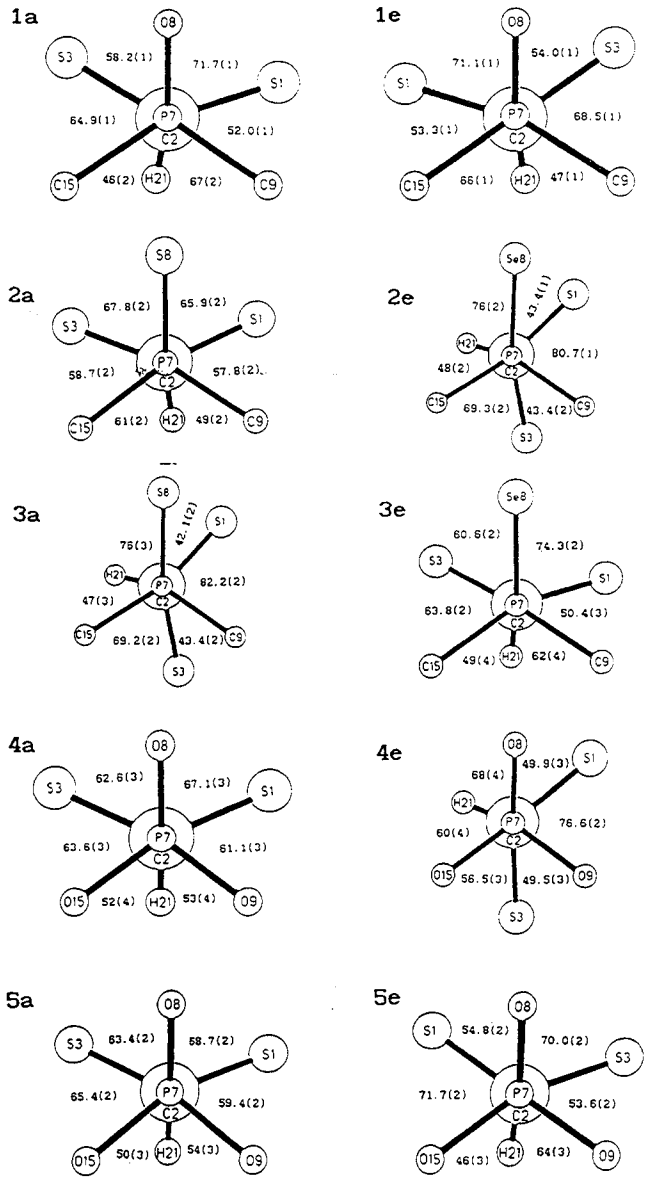

FIGURE 4 The Newman projections perpendicular to the P7–C2 bond in 1,3-dithianes **1–5**.

whole P7=S8 and P7=Se8 groups, so that the position of sulfur or selenium becomes synclinal to the hydrogen H21, with the torsion angles of 76(3)° and 76(2)°, respectively.

In Table 2, some bond lengths in the examined structures **1–5** are collected. Table 3 presents selected valence angles in the investigated compounds **1–5**. Their analysis points to an important influence of the P=X group on the values of endocyclic sulfur angles. These values are greater by 3.6°–5.4° for the axial compounds when compared with those for the respective equatorial ones, and the difference increases on going from **1** to **2** and **3** (the respective differences are as follows: 5.0°→5.4°→5.4°). The endocyclic angles S1–C2–S3

TABLE 2 Selected Bond Lengths (Å) in **1–5**

	1a	**2a**	**3a**	**4a**	**5a**
S1–C2	1.808(2)	1.801(3)	1.801(4)	1.801(5)	1.794(3)
C2–S3	1.806(2)	1.811(4)	1.805(4)	1.794(4)	1.809(3)
S3–C4	1.810(2)	1.811(4)	1.813(4)	1.805(4)	1.810(3)
C4–C5	1.524(3)	1.525(4)	1.525(5)	1.529(6)	1.529(4)
C5–C6	1.522(3)	1.535(5)	1.519(5)	1.523(4)	1.529(3)
C6–S1	1.812(2)	1.814(4)	1.797(4)	1.812(4)	1.805(3)
P7–C2	1.828(2)	1.825(3)	1.849(4)	1.799(4)	1.802(3)
P7–X8[a]	1.485(1)	1.946(1)	2.098(2)	1.460(3)	1.445(2)
P7–Y9[a]	1.805(2)	1.819(4)	1.819(4)	1.567(3)	1.582(3)
P7–Y15[b]	1.810(2)	1.820(3)	1.829(4)	1.565(6)	1.585(3)
S1..S3[b]	3.030(2)	3.054(3)	3.050(4)	3.003(4)	3.065(3)
	1e	**2e**	**3e**	**4e**	**5e**
S1–C2	1.800(2)	1.808(3)	1.816(2)	1.797(4)	1.813(2)
C2–S3	1.810(2)	1.805(3)	1.804(2)	1.796(4)	1.812(3)
S3–C4	1.810(3)	1.811(2)	1.800(3)	1.799(5)	1.820(3)
C4–C5	1.516(3)	1.531(4)	1.537(4)	1.517(6)	1.523(3)
C5–C6	1.524(3)	1.537(4)	1.524(4)	1.522(5)	1.511(4)
C6–S1	1.814(3)	1.809(2)	1.817(3)	1.805(5)	1.811(3)
P7–C2	1.818(2)	1.831(2)	1.840(3)	1.800(4)	1.801(3)
P7–X8[a]	1.485(2)	1.952(1)	2.104(1)	1.452(3)	1.451(2)
P7–Y9[a]	1.809(2)	1.818(4)	1.812(3)	1.567(4)	1.581(2)
P7–Y15[a]	1.799(2)	1.824(3)	1.813(2)	1.548(4)	1.585(2)
S1..S3[b]	2.988(2)	2.991(2)	2.992(2)	2.990(4)	3.042(3)

[a]X and Y are the following types of atoms:

	1a, e	**2a, e**	**3a, e**	**4a, e**	**5a, e**
X	O	S	Se	O	O
Y	C	C	C	O	O

[b]Nonbonding distance.

TABLE 3 Selected Valence Angles (°) in **1–5**

	1a	**2a**	**3a**	**4a**	**5a**
S1 C2 S3	114.0(1)	115.4(2)	115.5(2)	113.4(2)	116.6(2)
C2 S3 C4	102.3(1)	103.7(2)	104.1(2)	101.4(2)	102.3(1)
S3 C4 C5	114.7(1)	114.4(2)	115.0(3)	115.5(2)	112.7(2)
C4 C5 C6	109.0(2)	109.1(3)	108.9(3)	110.6(3)	107.9(2)
C5 C6 S1	114.6(1)	114.2(2)	115.5(3)	115.5(3)	113.1(2)
C6 S1 C2	102.1(1)	103.5(2)	103.2(2)	101.5(2)	102.5(1)
S1 C2 P7	114.2(1)	112.4(2)	114.1(2)	113.6(2)	112.7(2)
S3 C2 P7	110.4(1)	113.9(2)	113.2(2)	111.6(2)	110.2(2)
C2 P7 X8[a]	114.0(1)	114.8(1)	115.3(1)	115.9(2)	117.3(1)
C2 P7 Y9[a]	107.1(1)	103.6(2)	104.7(2)	101.8(2)	100.9(1)
C2 P7 Y15[a]	105.0(1)	106.6(2)	101.6(2)	105.1(2)	104.9(1)
X8 P7 Y9[a]	111.5(1)	112.9(1)	112.8(1)	117.1(2)	116.8(1)
X8 P7 Y9[a]	111.5(1)	112.9(1)	112.8(1)	117.1(2)	116.8(1)
Y9 P7 Y15[a]	106.6(1)	104.4(2)	106.7(2)	101.6(2)	99.7(1)
C4 C5 C21	112.9(2)	112.9(3)	112.7(3)	112.6(3)	114.4(2)
C6 C5 C21	113.0(2)	111.9(3)	113.2(3)	111.8(3)	113.1(2)
	1e	**2e**	**3e**	**4e**	**5e**
S1 C2 S3	111.7(1)	111.7(2)	111.5(1)	112.7(2)	114.1(1)
C2 S3 C4	97.5(1)	98.5(1)	98.7(1)	98.5(2)	98.9(1)
S3 C4 C5	115.6(2)	115.3(2)	115.3(2)	115.0(3)	113.8(2)
C4 C5 C6	110.6(2)	110.4(2)	109.8(2)	109.2(3)	109.1(2)
C5 C6 S1	115.0(2)	116.3(2)	116.5(2)	113.8(3)	114.4(2)
C6 S1 C2	97.0(1)	97.8(1)	97.7(1)	98.9(2)	98.6(1)
S1 C2 P7	114.6(1)	109.9(2)	109.3(1)	109.8(2)	108.9(1)
S3 C2 P7	107.9(1)	113.1(2)	112.1(1)	112.3(2)	108.8(1)
C2 P7 X8[a]	114.5(1)	111.5(1)	111.8(1)	112.8(2)	117.5(1)
C2 P7 Y9[a]	103.4(1)	106.8(1)	105.8(1)	103.0(2)	106.3(1)
C2 P7 Y15[a]	107.3(1)	106.9(1)	106.9(1)	106.1(2)	99.8(1)
X8 P7 Y9[a]	112.4(1)	113.3(1)	113.6(1)	116.6(2)	110.0(1)
X8 P7 Y15[a]	111.6(1)	112.4(1)	112.2(1)	115.5(2)	116.2(1)
Y9 P7 Y15[a]	107.2(1)	105.5(1)	106.1(1)	101.2(2)	105.9(1)
C4 C5 C21	112.2(2)	111.8(2)	112.7(2)	113.7(3)	113.2(2)
C6 C5 C21	113.2(2)	111.7(2)	111.4(2)	113.3(3)	113.4(2)

[a]X, Y, and Y are the following types of atoms:

	1a, e	**2a, e**	**3a, e**	**4a, e**	**5a, e**
X	O	S	Se	O	O
Y	C	C	C	O	O

describing the gaping of the hetero ring in **1–5**, ordered in two different ways, are as follows:

(1) for axial diastereomers:

1a, **2a**, **3a** (O→S→Se): 114.0°, 115.4°, 115.5°

4a, **1a**, **5a** (OMe→Ph→OCH_2CF_3): 112.7°, 111.7°, 114.1°.

(2) for equatorial diastereomers:

1e, **2e**, **3e** (O→S→Se): 111.7°, 111.7°, 111.5°

4e, **1e**, **5e** (OMe→Ph→OCH_2CF_3): 112.7°, 111.7°, 114.1°.

Comparing these angles in a set of pairs (axial-equatorial), we can see that the above-mentioned difference increases when the size of the P=X group becomes larger: 2.3°→3.7°→4.0° and 0.7°→2.3°→2.5° for **1**→**2**→**3** and **4**→**1**→**5**, respectively.

EXPERIMENTAL

Crystal and molecular structures of **1–5** were determined using data collected on a CAD4 diffractometer. The dithianes **2a**, **2e**, **3e**, and **5e** crystallize in the triclinic system, **3a**, **4a**, **5a**, **1e**, and **4e** in the monoclinic system, and only **1a** is orthorhombic. Crystal data and experimental details are collected in Tables 4 and 5. The thermal ellipsoidal drawings of molecules **1a–5e** are presented in Figure 5. Intensity data of all compounds were collected at room temperature using a diffractometer with graphite monochromatized radiation. Lattice constants were refined by a least-squares fit of 25 reflections in θ ranges: 13.3–38.4° (**1a**), 8.3–15.7° (**2a**), 10.0–15.6° (**3a**), 21.7–26.3° (**4a**), 22.1–27.6° (**5a**), 10.1–13.9° (**1e**), 10.5–15.2° (**2e**), 20.7–27.6° (**3e**), 21.7–24.6° (**4e**), and 18.8–28.5° (**5e**). Absorption corrections were performed in case of structures **4a**, **4e**, **5e**, by use of the DIFABS program [14,15], and in

TABLE 4 Crystal Data and Experimental Details for Axial Diastereomers **1a–5a**

	1a	**2a**	**3a**	**4a**	**5a**
Molecular formula	$C_{20}H_{25}OPS_2$	$C_{20}H_{25}PS_3$	$C_{20}H_{25}PS_2Se$	$C_{10}H_{21}O_3PS_2$	$C_{12}H_{19}O_3F_6PS_2$
M	376.49	392.55	439.45	284.38	388.38
Crystallographic system	orthorhombic	triclinic	monoclinic	monoclinic	monoclinic
Space group	Pbca	$P\bar{1}$	$P2_1/c$	$P2_1/n$	$P2_1/c$
a (Å)	18.879(1)	6.496(2)	9.634(5)	11.103(1)	5.826(1)
b (Å)	19.129(1)	10.836(2)	17.036(9)	11.088(1)	11.242(1)
c (Å)	11.212(1)	15.242(3)	13.342(4)	12.817(1)	28.520(4)
α (°)	(90)	100.60(2)	(90)	(90)	(90)
β (°)	(90)	91.38(2)	100.41(1)	110.64(1)	91.74(1)
γ (°)	(90)	99.56(2)	(90)	(90)	(90)
V (Å^3)	4049.2(6)	1038.79(1.5)	2153.8(1.8)	1477(1)	1867(1)
Z	8	2	4	4	4
D_c (g/cm^3)	1.235(2)	1.256(2)	1.355(2)	1.279(2)	1.382(2)
μ (cm^{-1})	31.3	4.2	19.8	42.2	38.9
Crystal dimensions (mm)	0.2, 0.5, 0.7	0.3, 0.5, 0.5	0.2, 0.5, 0.5	0.3, 0.4, 0.4	0.2, 0.4, 0.9
Maximum 2θ (°)	150	50	50	150	150
Radiation, λ (Å)	Cu Kα, 1.54178	MO Kα, 0.71069	MO Kα, 0.71069	Cu Kα, 1.54178	Cu Kα, 1.54178
Scan mode	$\omega/2\theta$	$\omega/2\theta$	$\omega/2\theta$	$\omega/2\theta$	$\omega/2\theta$
Scan width (°)	0.80 + 0.14 tanθ	0.80 + 0.35 tanθ	0.75 + 0.35 tanθ	0.80 + 0.14 tanθ	0.87 + 0.14 tanθ
hkl ranges	h = 0 23	h = 0 7	h = 0 11	h = 0 13	h = −7 0
	k = 0 23	k = −12 12	k = 0 20	k = 0 13	k = 0 14
	l = 0 14	l = −15 15	l = −15 15	l = −16 14	l = −35 35
No. of reflections:					
unique	3899	3450	3516	3007	4026
with $I \geq 3\sigma(I)$	3623	3164	3318	2688	3664
No. of parameters refined	318	317	217	146	217
Largest differential peak (eÅ^{-3})	0.471	0.396	0.826	0.669	0.554
R	0.0416	0.0425	0.0465	0.0766	0.0659
R_w	0.0525	0.0466	0.0497	0.1071	0.0868
Weighting coefficient[a] **g**	0.002882	0.000504	0.003895	0.002686	0.004148
Extinction parameter	0.00826(63)	—	—	0.0051(24)	—
Absorption correction: min.	—	—	—	0.7902	—
max.	—	—	—	1.1455	—
aver.	—	—	—	1.0054	—
Intensity correction: min.	—	1.00001	1.00006	0.9479	1.00026
max.	—	1.01824	1.06858	1.0263	1.11672
aver.	—	1.00838	1.03368	0.9874	1.05478

[a]Weighting scheme was $W = 1/(\sigma^2(F) + \mathbf{g}^* F^2)$.

TABLE 5 Crystal Data and Experimental Details for Equatorial Diastereomers **1e–5e**

	1e	**2e**	**3e**	**4e**	**5e**
Molecular formula	$C_{20}H_{25}OPS_2$	$C_{20}H_{25}PS_3$	$C_{20}H_{25}PS_2Se$	$C_{10}H_{21}O_3PS_2$	$C_{12}H_{19}O_3F_6PS_2$
M	376.49	392.55	439.45	284.38	388.38
Crystallographic system	monoclinic	triclinic	triclinic	monoclinic	triclinic
Space group	$P2_1/c$	$P\bar{1}$	$P\bar{1}$	$P2_1/c$	$P\bar{1}$
a (Å)	10.027(2)	9.594(2)	9.6498(9)	17.100(2)	5.696(1)
b (Å)	18.731(2)	9.712(2)	9.9377(4)	9.530(1)	10.935(1)
c (Å)	11.139(4)	12.378(3)	12.2167(7)	9.210(1)	15.008(1)
α (°)	(90)	74.61(1)	111.066(5)	(90)	79.03(1)
β (°)	106.28(2)	67.57(1)	103.219(6)	96.55(1)	84.87(1)
γ (°)	(90)	84.11(2)	95.788(6)	(90)	86.89(1)
V (Å^3)	2008.2(1.7)	1027.8(1.0)	1042.5(3.2)	1491(1)	913(1)
Z	4	2	2	4	2
D_c (g/cm^3)	1.245(2)	1.265(2)	1.400(2)	1.287(2)	1.412(2)
μ (cm^{-1})	3.4	39.8	50.6	41.8	39.8
Crystal dimensions (mm)	0.3, 0.3, 0.7	0.2, 0.4, 0.6	0.3, 0.5, 0.5	0.2, 0.3, 0.8	0.3, 0.4, 0.6
Maximum 2θ (°)	50	120	150	150	150
Radiation, λ (Å)	Mo Kα, 0.71069	Cu Kα, 1.54178	Cu Kα, 1.54178	Cu Kα, 1.54178	Cu Kα, 1.54178
Scan mode	$\omega/2\theta$	$\omega/2\theta$	$\omega/2\theta$	$\omega/2\theta$	$\omega/2\theta$
Scan width (°)	0.70 + 0.35 tanθ	0.60 + 0.14 tanθ	0.77 + 0.14 tanθ	1.05 + 0.14 tanθ	0.80 + 0.14 tanθ
hkl ranges	h = 0 11	h = −9 10	h = 0 12	h = 0 21	h = 0 7
	k = 0 22	k = −10 10	k = −12 12	k = 0 11	k = −13 13
	l = −13 12	l = 0 13	l = −15 14	l = −11 11	l = −18 18
No. of reflections:					
unique	3403	3077	4500	2845	4013
with $I \geq 3\sigma(I)$	3215	2924	4236	2826	3642
No. of parameters refined	317	218	218	146	218
Largest differential peak (eÅ^{-3})	0.406	0.352	0.593	0.376	0.382
R	0.0388	0.0431	0.0409	0.0684	0.0550
R_w	0.0425	0.0599	0.0585	0.1053	0.0834
Weighting coefficient[a] **g**	0.000182	0.004486	0.002907	0.003052	0.001429
Extinction parameter	—	0.0237(33)	0.0234(25)	0.0022(19)	0.0084(31)
Absorption correction: min.	—	0.8273	—	0.6204	0.6928
max.	—	0.9983	—	1.2333	1.3112
aver.	—	0.9286	—	0.9379	0.9735
Intensity correction: min.	—	—	—	1.00002	1.00005
max.	—	—	—	1.09795	1.05087
aver.	—	—	—	1.03199	1.02449

[a]Weighting scheme was $W = 1/(\sigma^2(F) + \mathbf{g}^* F^2)$.

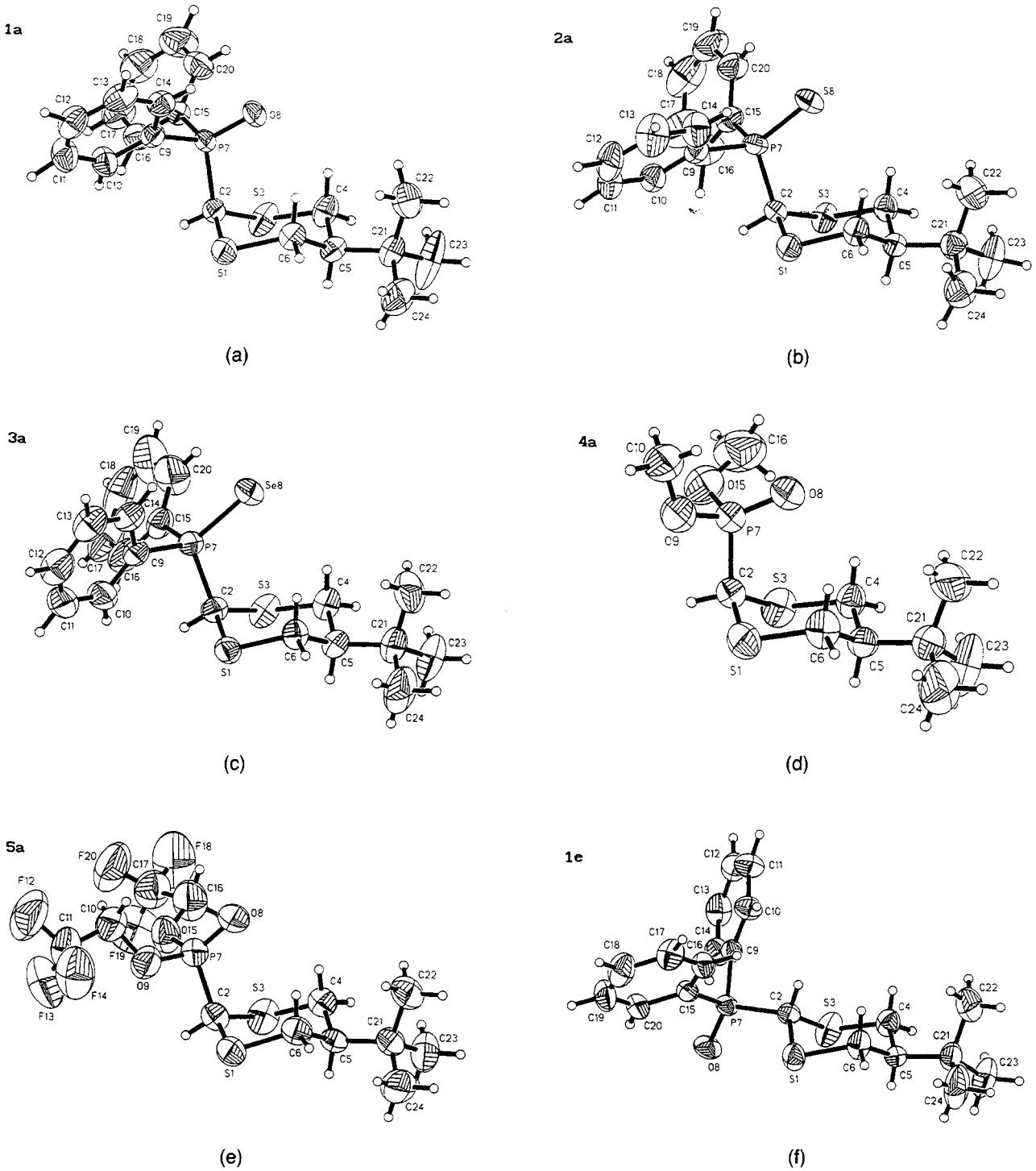

FIGURE 5 Thermal ellipsoidal plots with the atom numbering schemes of the molecules of (a) **1a**, (b) **2a**, (c) **3a**, (d) **4a**, (e) **5a**, (f) **1e**, (g) **2e**, (h) **3e**, (i) **4e**, and (j) **5e**.

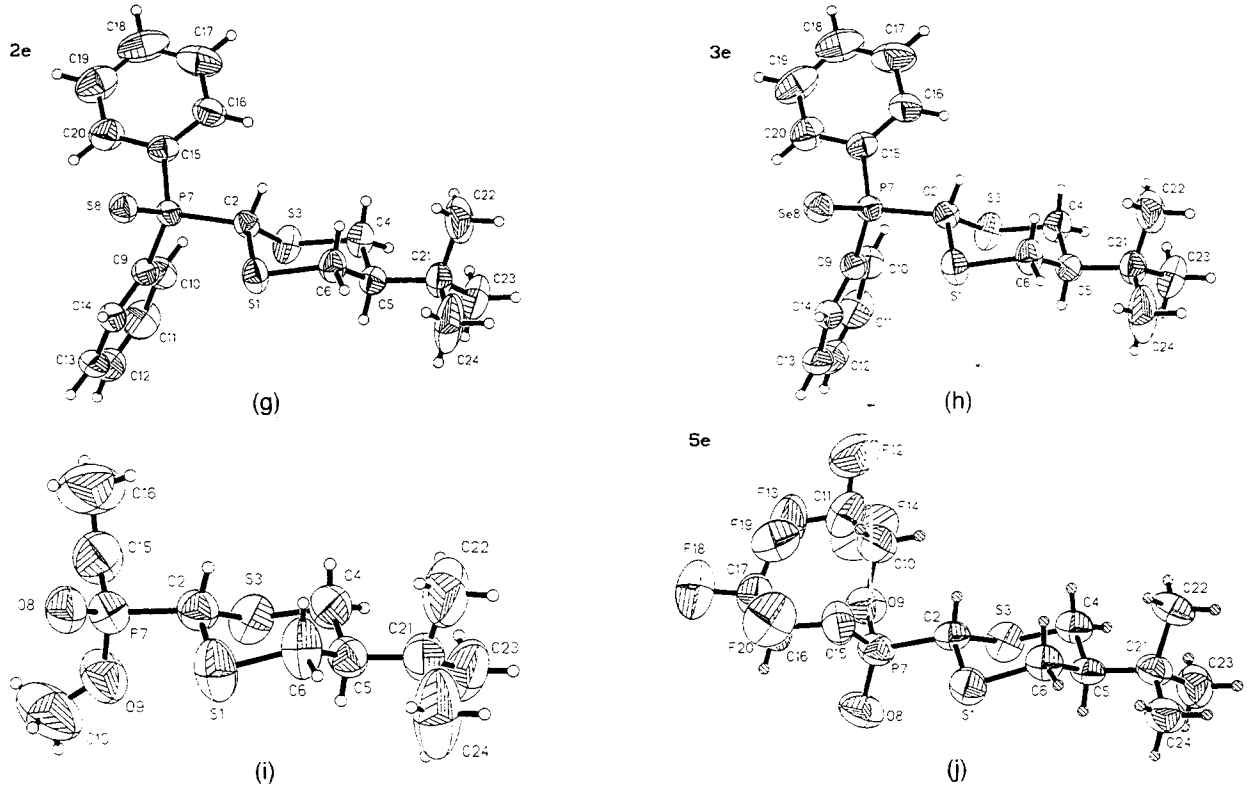

FIGURE 5 (continued) Thermal ellipsoidal plots with the atom numbering schemes of the molecules of (a) **1a**, (b) **2a**, (c) **3a**, (d) **4a**, (e) **5a**, (f) **1e**, (g) **2e**, (h) **3e**, (i) **4e**, and (j) **5e**.

2e, by use of the EAC program [14,16]. Because the decline in intensities of three standard reflections was observed during the exposure time, the intensity correction was applied for **2a**, **3a**, **5a**, **4e**, and **5e**, by use of the DECAY program [14], and for **4a**, by use of the CHORT program [14]. Data corrections were performed with the Enraf-Nonius SDP crystallographic computing package [14]. All structural calculations of **1a–5e** were performed with the SHELXTL [17] package. In all structures, in order to solve them by direct methods and to refine them by full matrix least-squares using Fs [18], the observed reflections with $I \geq 3\sigma(I)$ were used. In structure **1a**, **1e**, and **2a**, the hydrogen atoms were found on a difference map and were refined isotropically. In the remaining structures, hydrogens were placed geometrically, set as riding with the isotropic thermal parameters fixed as 1.3 times that of the equivalent isotropic thermal parameter of the corresponding parent-atom and not refined. Anisotropic thermal parameters were refined for all nonhydrogen atoms in all structures. The all structural refinements were performed using the weighting scheme $1/(\sigma^2(F) + g^*F^2)$ (see Tables 4 and 5). Full crystallographic data of **1a–5e** and values of F_{obs}, F_{calc} are deposited at the Cambridge Crystallographic Data Centre [19].

ACKNOWLEDGMENT

This work was financially supported by the State Committee for Scientific Research (KBN), Grant No. 2-0696-91-01.

REFERENCES

[1] P. v. R. Schleyer, E. D. Jemmis, G. W. Spitznagel, *J. Am. Chem. Soc.*, *107*, 1985, 6393.

[2] (a) U. Salzner, P. v. R. Schleyer, *J. Chem. Soc., Chem. Comm.*, 1990, 190; (b) B. M. Pinto, J. Sandoval-Ramirez, R. Dev Sharma, A. C. Willis, F. W. B. Einstein, *Can. J. Chem.*, *64*, 1986, 732.

[3] E. Juaristi, *Heteroatom Chem.*, *1*, 1990, 267.

[4] (a) M. Mikołajczyk, *Pure Appl. Chem.*, *57*, 1987, 983; (b) M. Mikołajczyk, P. Graczyk, P. Bałczewski, *Tetrahedron Lett.*, *28*, 1987, 573; (c) M. Mikołajczyk, P. Graczyk, M. I. Kabachnik, A. P. Baranov, *J. Org. Chem.*, *54*, 1989, 2859; (d) M. Mikołajczyk, P. Graczyk, M. W. Wieczorek, G. Bujacz, *Angew. Chem.*, *103*, 1991, 604; *Angew. Chem. Int. Ed. Engl.*, *30*, 1991, 578.

[5] A. J. Kirby: *The Anomeric Effect and Related Stereoelectronic Effects at Oxygen*, Springer-Verlag, Berlin, 1983.

[6] K. B. Wiberg, M. A. Murcko, *J. Am. Chem. Soc.*, *111*, 1989, 4821.

[7] (a) A. Cosse-Barbi, J. E. Dubois, *J. Am. Chem. Soc.*, *109*, 1987, 1503; (b) A. Cosse-Barbi, D. G. Watson,

J. E. Dubois, *Tetrahedron Lett., 30,* 1989, 163; (c) J. E. Dubois, A. Cosse-Barbi, D. G. Watson, *Tetrahedron Lett., 30,* 1989, 167.

[8] (a) E. Juaristi, B. A. Valenzuela, L. Valle, A. T. McPhail, *J. Org. Chem., 49,* 1984, 3026; (b) E. Juaristi, L. Valle, B. A. Valenzuela, M. A. Aguilar, *J. Am. Chem. Soc., 108,* 1986, 2000.

[9] (a) B. Młotkowska, H. Gross, B. Costisella, M. Mikołajczyk, S. Grzejszczak, A. Zatorski, *J. Prakt. Chem., 319,* 1977, 17. (b) H. Gross, I. Keitel, B. Costisella, M. Mikołajczyk, and W. Midura, *Phosphorus and Sulfur, 16,* 1983, 257.

[10] M. Mikołajczyk, P. Bałczewski, K. Wróblewski, J., Karolak-Wojciechowska, A. Miller, M. W. Wieczorek, M. Y. Antipin, Y. T. Struchkov, *Tetrahedron, 40,* 1984, 4855.

[11] M. Engelhardt, G. Hägele, M. Mikołajczyk, P. Bałczewski, D. Wendisch, *Magn. Res. Chem., 23,* 1985, 18.

[12] M. Mikołajczyk, P. Bałczewski, M. W. Wieczorek, G. Bujacz, M. Y. Antipin, Y. T. Struchkov, *Phosphorus and Sulfur, 37,* 1988, 189.

[13] M. Mikołajczyk, P. P. Graczyk, M. W. Wieczorek, *J. Org. Chem., 59,* 1994, 1672.

[14] B. A. Frenz: *SDP—Structure Determination Package,* Enraf-Nonius, Delft, Holland, 1984.

[15] N. Walker, D. Stuart, *Acta Crystallogr, A39,* 1983, 159.

[16] A. C. T. North, D. C. Phillips, F. S. Mathews, *Acta Crystallogr., A24,* 1968, 351.

[17] *SHELXTL PC, Release 4.1* (May 1990). Siemens Analytical X-Ray Instruments, Inc., Madison, WI.

[18] *International Tables for X-Ray Crystallography,* The Kynoch Press, Birmingham, England, 1974.

[19] University Chemical Laboratory, Cambridge Crystallographic Data Centre, Lensfield Road, Cambridge CB2 1EW, United Kingdom.